Journal of Thermal Analysis and Calorimetry (2019) 137:1919–1928
https://doi.org/10.1007/s10973-019-08116-9

Hydration mechanisms of composite binders containing copper slag at different temperatures

Jin Liu[1] · Runhua Guo[1] · Pengcheng Shi[1] · Lei Huang[1]

Received: 2 September 2018 / Accepted: 15 February 2019 / Published online: 2 March 2019

Abstract
The hydration mechanisms of composite binders containing copper slag at different temperatures (20 °C and 50 °C) were investigated by hydration heat determination, TG/DTG, non-evaporable water content measurement and X-ray diffraction (XRD). The compressive strengths of mortars containing copper slag cured at different temperatures were also determined. In addition to plain cement, quartz powder with a similar particle size and the same replacement ratio as copper slag was selected as the control sample. The results show that the addition of quartz powder has a slight acceleration effect on the hydration of cement, while the addition of copper slag has a strong retarding effect on the hydration of cement. The second exothermic peak of the composite binder containing copper slag is delayed as the copper slag content increases, but this trend weakens at high temperatures. The hydration heat of the composite binder containing copper slag decreases with increasing copper slag addition. Moreover, the hydration heat of the composite binder containing copper slag is higher than that of the composite binder containing an equal mass of quartz powder within 72 h. Copper slag has pozzolanic activity and consumes $Ca(OH)_2$ in hardened paste, although the pozzolanic activity of copper slag is low. However, the pozzolanic activity of copper slag is enhanced at high temperature. Furthermore, the reaction of copper slag does not produce new crystalline products compared to those produced by cement. Moreover, compared to hardened plain cement, the hardened composite binder containing copper slag has a higher non-evaporable water content gain rate. The mortar containing copper slag also has a higher compressive strength gain rate than the mortar containing equal mass quartz powder. Although the compressive strength of mortar containing copper slag is lower than that of plain cement mortar, it is higher than that of mortar containing quartz powder.

Keywords Copper slag · Hydration heat · TG/DTG · Compressive strength · High temperature

Introduction

Mineral admixtures such as fly ash, silica fume, phosphorus slag, ground granulated blast-furnace slag (GGBS) and limestone powder are widely used in cement-based materials. Accordingly, an increasing number of studies have investigated the hydration mechanisms of mineral admixtures in composite binders. The addition of a mineral admixture, including quartz powder, increases the actual water-to-cement ratio and provides more space for the hydration product of cement, which is called the dilution effect and can accelerate cement hydration [1, 2]. In addition, the filling effect of a mineral admixture can refine the pore structure of hardened paste [3–5]. Some mineral admixtures, such as GGBS and steel slag, also have hydraulic activity and produce C-S–H gels [5, 6]. Moreover, many mineral admixtures, such as fly ash, silica fume and phosphorus slag, have pozzolanic activity; thus, they participate in the reaction process in which $Ca(OH)_2$ is consumed and C-S–H gel is produced [7–9]. Both the hydraulic reaction and pozzolanic reaction of mineral admixtures are beneficial to the microstructure of concrete [10–12]. However, the hydration activity of composite binder containing mineral admixtures is relatively low, and the hydration activity of concrete containing mineral admixtures is obviously lower than that of plain concrete at early ages [13, 14]. High temperature can promote the

✉ Runhua Guo
guorh@tsinghua.edu.cn

[1] Department of Civil Engineering, Tsinghua University, Beijing 100084, China

hydration activity of cement as well as mineral admixtures, and concrete containing mineral admixtures subjected to high-temperature curing can achieve satisfactory early compressive strength [15–18].

In the production of copper, the output of copper slag, a by-product of the process, is approximately double the copper output [19, 20]. The major chemical compositions of copper slag are Fe_2O_3, SiO_2, Al_2O_3, CaO, MgO and SO_3 [21, 22]. Influenced by the raw materials used and temperature history, the common mineral components of copper slag include fayalite, anorthite, magnetite and glass phase [23–25]. Research on the application of copper slag has focused on recovering metal from copper slag [26–28], on using copper slag as an aggregate in asphalt mixture [29, 30], and on using copper slag as a fine aggregate in cement concrete [31–33]. Similar to blast-furnace slag and steel slag, copper slag exhibits reactivity after being ground to powder, so the utilization of copper slag as a mineral admixture in concrete has also been reported in some studies [34, 35]. Owing to the low water absorption of copper slag, fresh concrete containing copper slag has better fluidity than concrete without copper slag [36, 37]. The compressive strength of concrete containing copper slag decreases as the amount of copper slag added increases at all ages, especially when the copper slag addition is more than 30% [38, 39]. However, the compressive strength of concrete containing copper slag under sulfate attack is higher than that of the concrete without copper slag under sulfate attack [39]. In another study, the addition of copper slag did not decrease the compressive strength or split the tensile strength of concrete [40]. Furthermore, the carbonization depth and absorption of concrete containing copper slag are less than those of concrete without copper slag [40]. Although the performance of concrete containing copper slag has been investigated in some studies, the discussion about the hydration properties of the composite binder containing copper slag is limited.

In this paper, the hydration mechanism of composite binder containing copper slag was investigated by determining the hydration heat, $Ca(OH)_2$ content, non-evaporable water content, mineral phase and compressive strength. Considering the dilution effect, nucleation effect and filling effect of copper slag, quartz powder with a similar particle size and the same replacement ratio as copper slag was selected as the control sample. The influence of curing temperature on the hydration of the composite binder containing copper slag is also discussed.

Raw materials and test methods

The cement used was Portland cement with a strength grade of 42.5, which is compliant with the Chinese National Standard GB175-2007. Table 1 shows the chemical compositions of the cement and copper slag. The X-ray diffraction (XRD) pattern of the copper slag is shown in Fig. 1. Figure 2 shows particle sizes of the copper slag and quartz powder. The coarse aggregate was crushed

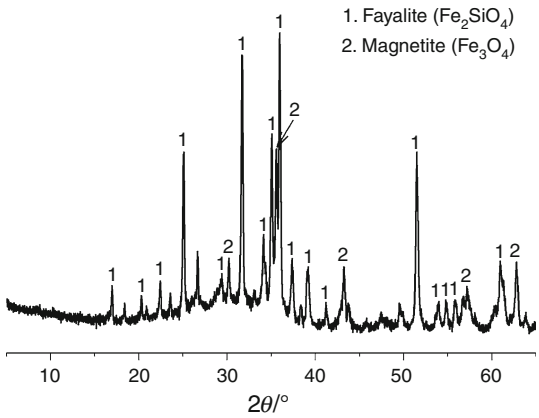

Fig. 1 XRD pattern of the copper slag

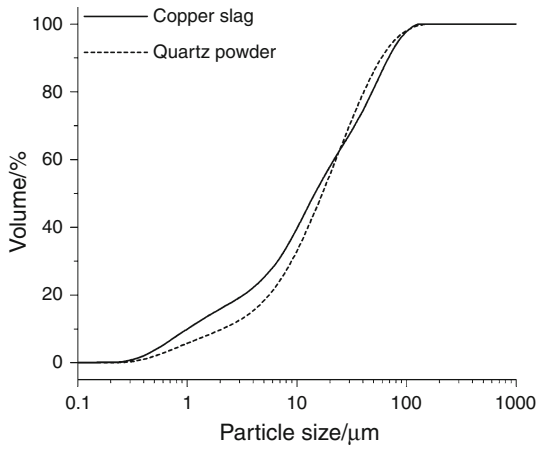

Fig. 2 Particle sizes of the copper slag and quartz powder

Table 1 Chemical compositions of the cement and copper slag (%)

Sample	SiO_2	Al_2O_3	Fe_2O_3	CaO	MgO	ZnO	SO_3	Na_2O_{eq}
Cement	17.93	4.28	3.41	67.52	1.94	–	3.46	0.66
Copper slag	35.24	9.99	42.57	3.20	1.76	2.35	2.58	0.98

$Na_2O_{eq} = Na_2O + 0.685K_2O$

Table 2 Mix proportions of pastes (g)

Sample	Cement	Copper slag	Quartz powder	Water
C	100	–	–	40
S1	85	15	–	40
Q1	85	–	15	40
S2	70	30	–	40
Q2	70	–	30	40
S3	55	45	–	40
Q3	55	–	45	40

Table 3 Mix proportions of mortars (g)

Sample	Cement	Copper slag	Quartz powder	Sand	Water
C	450	–	–	1350	180
S1	382.5	67.5	–	1350	180
Q1	382.5	–	67.5	1350	180
S2	315	135	–	1350	180
Q2	315	–	135	1350	180
S3	247.5	202.5	–	1350	180
Q3	247.5	–	202.5	1350	180

limestone between 5 and 25 mm. The fine aggregate was natural river sand smaller than 5 mm.

The mix proportions of pastes and mortars are shown in Tables 2 and 3, respectively. An isothermal calorimeter was used to collect the exothermic rates and cumulative hydration heats of plain cements and composite binders at constant temperatures of 20 °C and 50 °C. The pastes were mixed and then poured into plastic sealed tubes to prevent carbonization and water loss. At different testing ages, the hardened pastes were removed and then soaked in absolute alcohol to prevent further hydration. The mineral phases of the hardened pastes were determined by XRD. A thermal analyzer was used to collect the TG/DTG curves of the hardened pastes, and the $Ca(OH)_2$ contents of the hardened pastes were calculated from the TG/DTG curves at the ages of 28 d and 60 d. The non-evaporable water contents of the hardened pastes at the ages of 3 d, 7 d, 28 d and 60 d were measured by calculating the mass loss of the hardened pastes between 105 °C and 1000 °C. Mortars of 40 × 40 × 160 mm were cast. The compressive strength of the mortar was measured at ages of 3 d, 7 d, 28 d and 60 d.

Two curing conditions were adopted in this research: standard curing and high-temperature curing. For standard curing, the samples were cured in a curing box at a temperature of 20 ± 1 °C and a relative humidity (RH) not less than 95%. For high-temperature curing, the samples were cured in a curing box at a temperature of 50 ± 1 °C for 7 d and then cured under the standard curing conditions. The standard curing and high-temperature curing are denoted with the suffixes "-N" and "-H", respectively.

Result and discussion

Hydration heat

Figure 3a shows the exothermic rate curves of plain cements and composite binders at 20 °C. The second exothermic peak value of the binder decreases as the replacement ratio of cement by copper slag increases, which indicates that the hydration activity of copper slag is obviously lower than that of cement at early ages. The time of the second exothermic peak increased slightly with increasing quartz powder content. This acceleration effect is attributable to the nucleation effect and dilution effect (increased actual water-to-cement ratio) of quartz powder [14, 15]. Because of the amount of particles with small size (≤ 20 μm) of copper slag is higher than that of quartz powder, the nucleation effect of copper slag should be a little stronger than that of quartz powder. However, the time of the second exothermic peak is delayed with the increase in copper slag content. In particular, when the cement replacement ratio is 45%, the second exothermic peak of the composite binder containing copper slag is approximately 8 h later than that of plain cement. These results indicate that although copper slag also has a nucleation effect and dilution effect on the hydration of cement, copper slag also exhibits a retarding effect on cement hydration, and the retarding effect becomes stronger with increasing copper slag content. This may because some metal ions such as Zn in copper slag dissolve in cement paste, which have retarding effects on the hydration of cement [41, 42].

Figure 3b, c shows the cumulative hydration heat curves and cumulative heats, respectively, of plain cement and composite binders within 72 h at 20 °C. The cumulative hydration heat of the composite binder containing copper slag decreases as the amount of copper slag added increases at every stage within 72 h, which is due to the low reactivity of copper slag and the reduction in cement dosage. Furthermore, the cumulative hydration heat of the composite binder containing 15% quartz powder is higher than the 85% cumulative hydration heat of the plain cement, and similar results are obtained when the cement replacement ratio is 30% and 45%. These results also demonstrate the acceleration of the hydration of cement by quartz powder because of its nucleation effect and dilution effect. Notably, due to the acceleration effect of quartz

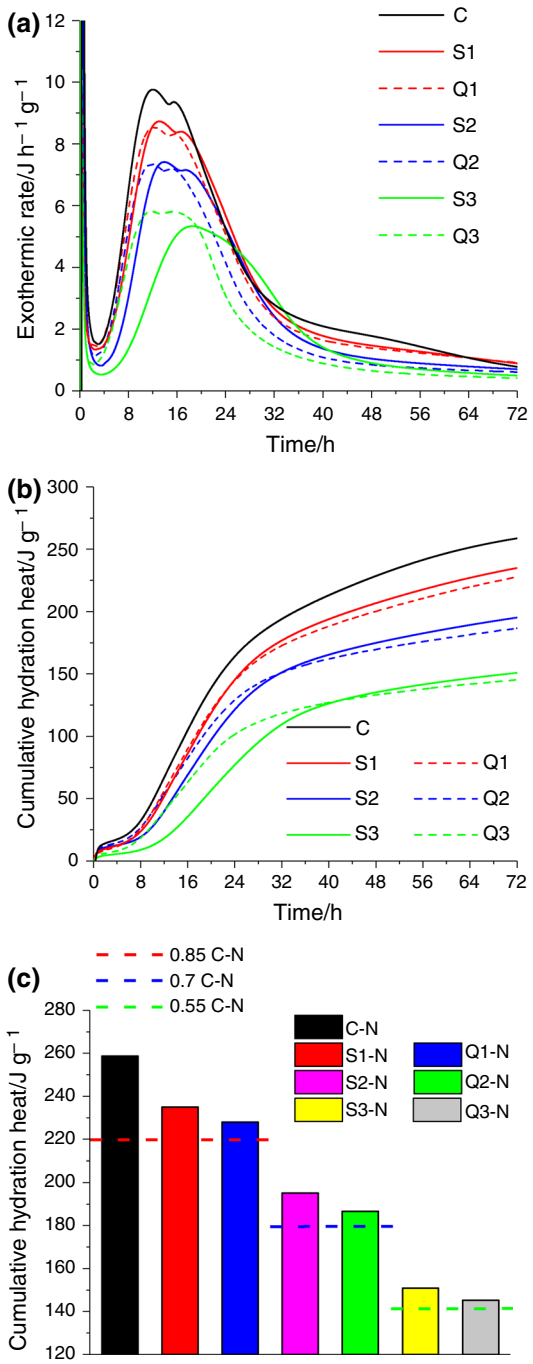

Fig. 3 **a** Exothermic rate curves of plain cement and composite binders at 20 °C. **b** Cumulative hydration heat curves of plain cement and composite binders at 20 °C. **c** Cumulative heat of plain cement and composite binders within 72 h at 20 °C

powder and the retarding effect of copper slag on the hydration of cement, the initial cumulative heat of the composite binder containing copper slag is lower than that of the composite binder containing an equal mass of quartz powder. However, the cumulative hydration heat curve of composite binder containing copper slag caught up with the cumulative hydration heat curve of composite binder containing equal mass quartz powder, and the cumulative hydration heat of composite binder containing copper slag is higher than of composite binder containing equal mass quartz powder within 72 h. These results indicate that copper slag has reacted partly and contributes to the hydration heat of the composite binder within 72 h.

Figure 4a shows the exothermic rate curves of plain cement and composite binders at 50 °C. The reactivities of plain cement and composite binders are promoted by high temperature, and compared with those at 20 °C, their secondary exothermic peak values at high temperature increase dramatically. Moreover, similar to the situation at 20 °C, the time of the second exothermic peak of the composite binder containing copper slag at 50 °C is delayed with the increase in copper slag content. However, compared with the time gaps observed at 20 °C, the time gaps between the second exothermic peaks for different composite binders containing copper slag at 50 °C shorten significantly. The retarding effect of copper slag on the hydration of cement also weakens at high temperature.

Figure 4b, c shows the cumulative hydration heat curves and cumulative heats, respectively, of plain cement and composite binders within 72 h at 50 °C. The cumulative heats of plain cement and composite binders at 50 °C are dramatically higher than those at 20 °C within 72 h, which also demonstrates the acceleration effect of high temperature on the reactivities of cement and composite binders. Moreover, the cumulative hydration heat of the composite binder containing 15% quartz powder is higher than the 85% cumulative hydration heat of the plain cement, and this phenomenon is more apparent than that observed at 20 °C. These results indicate that the acceleration effect (nucleation effect and dilution effect) of quartz powder is enhanced at high temperature. Furthermore, the cumulative hydration heat curve of composite binder containing copper slag caught up with the cumulative hydration heat curve of composite binder containing equal mass quartz powder, and the cumulative hydration heat of the composite binder containing copper slag is still higher than that of the composite binder containing equal mass quartz powder. These results indicate that copper slag has reacted partly and contributes to the hydration heat of the composite binder within 72 h at 50 °C.

TG/DTG results

Figure 5a, b shows the TG-DTG curves of the hardened pastes C-N, S2-N and Q2-N at ages of 28 d and 60 d, respectively. The TG-DTG results show the mass changes of the hardened pastes at elevated temperature. Every DTG curve displays an endothermic peak at approximately 350–500 °C, which represents the decomposition of

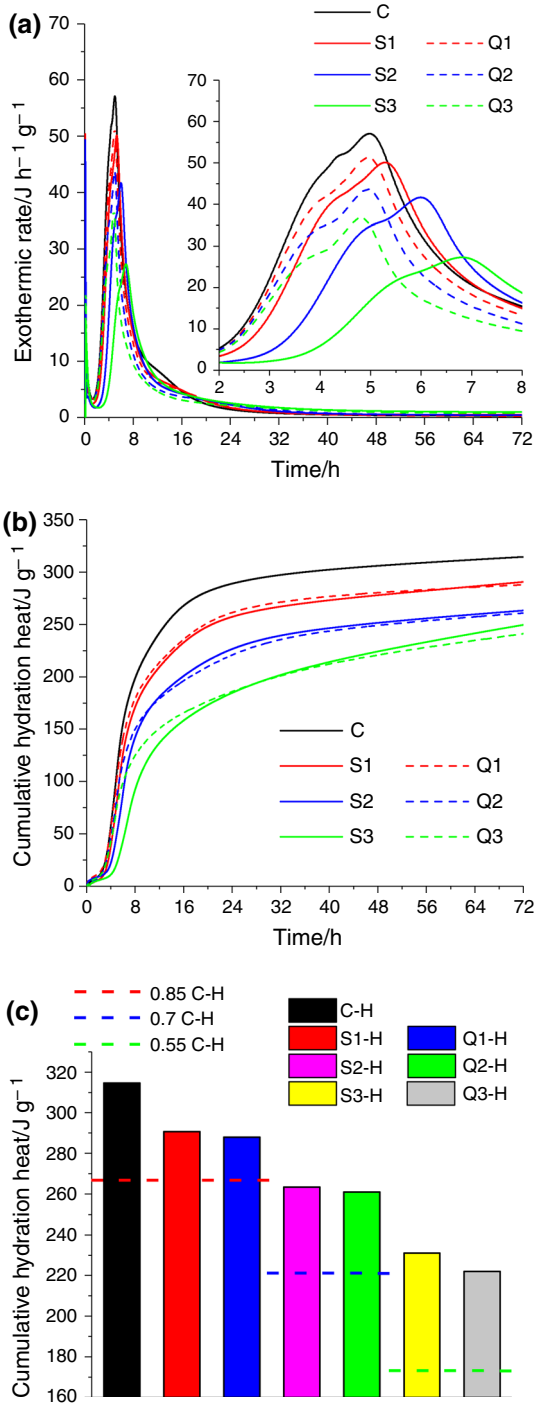

Fig. 4 **a** Exothermic rate curves of plain cement and composite binders at 50 °C. **b** Cumulative hydration heat curves of plain cement and composite binders at 50 °C. **c** Cumulative heat of plain cement and composite binders within 72 h at 50 °C

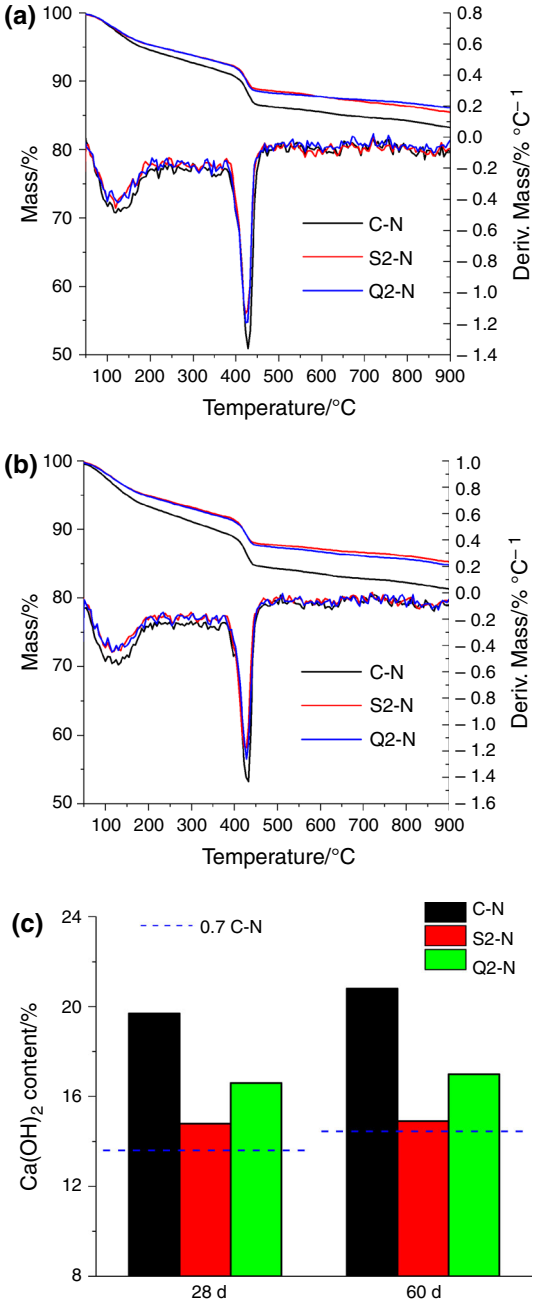

Fig. 5 **a** TG-DTG curves of hardened pastes C-N, S2-N and Q2-N at 28 d. **b** TG-DTG curves of hardened pastes C-N, S2-N and Q2-N at 60 d. **c** $Ca(OH)_2$ contents of hardened pastes C-N, S2-N and Q2-N

$Ca(OH)_2$ in the hardened paste. From the TG-DTG results, the $Ca(OH)_2$ contents of the hardened pastes are calculated and are shown in Fig. 5c. The $Ca(OH)_2$ content of hardened paste Q2-N is obviously lower than that of hardened paste C-N but is higher than the 70% $Ca(OH)_2$ content of hardened paste C-N. This result indicates that the dilution effect of quartz powder provides more space for cement hydration products, which elevates the hydration degree of the cement. Notably, the $Ca(OH)_2$ content of hardened paste S2-N is lower than that of hardened paste Q2-N, which indicates that the hydration of the copper slag consumes $Ca(OH)_2$. Thus, similar to fly ash, GGBS and silica fume, copper slag is a pozzolanic material, although its pozzolanic activity is relatively low (according to Fig. 4c).

Furthermore, the gap in $Ca(OH)_2$ content between hardened paste C-N and hardened paste S2-N increases from 28 d to 60 d. This result is attributable to the pozzolanic reaction of copper slag at late ages.

Figure 6a, b shows the TG-DTG curves of hardened pastes C-H, S2-H and Q2-H at ages of 28 d and 60 d, respectively. From the TG-DTG results, the $Ca(OH)_2$ contents of the hardened pastes are calculated and are shown in Fig. 6c. The $Ca(OH)_2$ content of hardened paste Q2-H is higher than the 70% $Ca(OH)_2$ content of hardened paste C-H, which is consistent with the results for the hardened pastes cured at 20 °C. Notably, the $Ca(OH)_2$ content of hardened paste S2-H is not only lower than that of hardened paste Q2-H but also lower than the 70% $Ca(OH)_2$ content of hardened paste C-H at 28 d and 60 d. These results indicate that the pozzolanic activity of copper slag is promoted by high temperature at early ages and that more $Ca(OH)_2$ is consumed by copper slag.

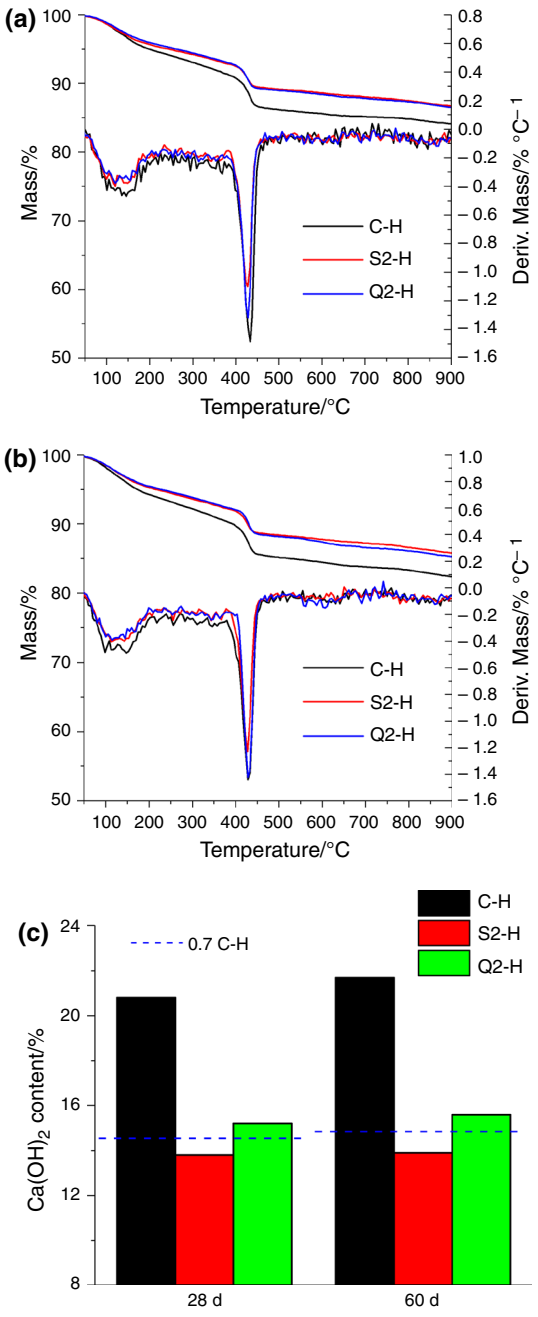

Fig. 6 **a** TG-DTG curves of hardened pastes C-H, S2-H and Q2-H at 28 d. **b** TG-DTG curves of hardened pastes C-H, S2-H and Q2-H at 60 d. **c** $Ca(OH)_2$ contents of hardened pastes C-H, S2-H and Q2-H

XRD

Figures 7–9 show XRD patterns of hardened pastes at ages of 3, 28 and 60 d, respectively. XRD is used to identify the crystalline substances in the hardened pastes. Compared to hardened plain cement, the composite binders containing copper slag and quartz powder exhibit different characteristic peaks corresponding to fayalite and SiO_2, respectively. These substances are mineral components of the raw materials. This result indicates that the reaction of copper slag does not produce new crystalline substances compared to those produced by cement. Moreover, at the age of 3 d, the characteristic peak of $Ca(OH)_2$ in the hardened paste cured at high temperature is stronger than that of $Ca(OH)_2$ in the hardened paste cured under standard curing conditions. Additionally, the characteristic peaks of AFm exist in the XRD patterns of the hardened plain cement and hardened composite binder containing copper slag cured at high temperature, while they do not exist in those cured under standard curing conditions. These results also imply that the hydration activities of plain cement and composite binder are promoted by high temperatures at early ages.

Non-evaporable water content

Figure 10a shows the non-evaporable water contents of hardened pastes under standard curing conditions. The non-evaporable water content represents the amount of hydration products, which relates to the hydration degree of the composite binder. Due to the retarding effect of copper slag and the acceleration effect of quartz powder on the hydration of cement, the non-evaporable water of the composite binder containing copper slag is lower than that of the composite binder containing an equal mass of quartz powder at early ages. However, the non-evaporable water content of the composite binder containing copper slag has a higher gain rate and is obviously higher than that of the composite binder containing an equal mass of quartz powder at late ages. Furthermore, the non-evaporable water content of the composite binder decreases as the replacement ratio of cement by copper slag increases at all ages. These results also show that the copper slag has low

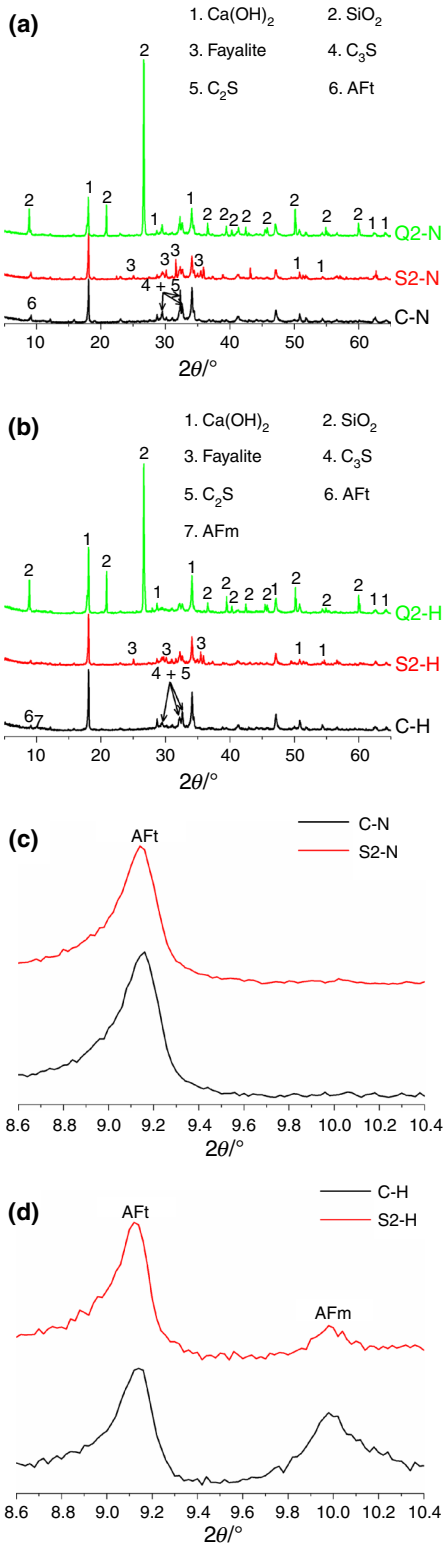

Fig. 7 XRD patterns of hardened pastes at 3 d. **a** standard curing; **b** high-temperature curing; **c** part of (**a**); **d** part of (**b**)

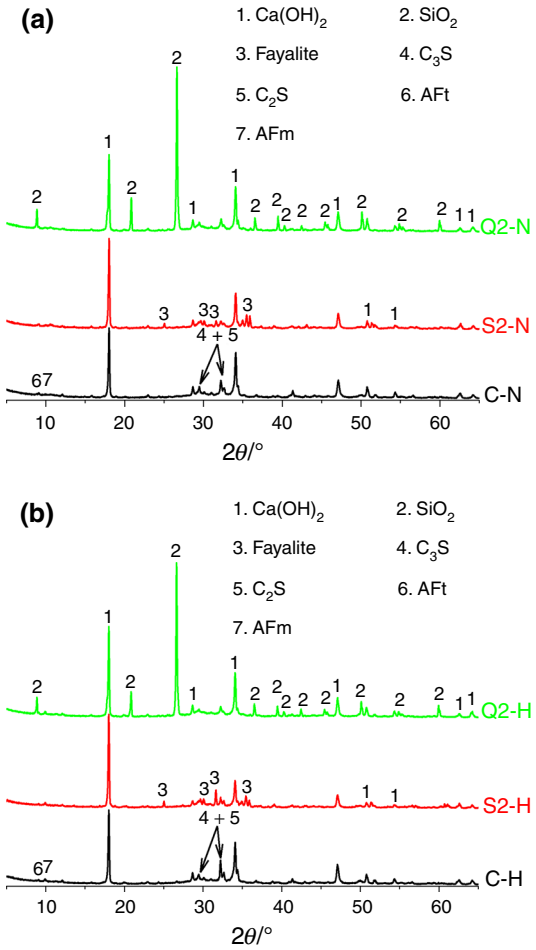

Fig. 8 XRD patterns of hardened pastes at 28 d. **a** standard curing; **b** high-temperature curing

hydration activity, which is consistent with the hydration heat and TG/DTG results.

Figure 10b shows the non-evaporable water contents of hardened pastes under high-temperature curing conditions. The non-evaporable water contents of the hardened pastes cured at 50 °C are obviously higher than those of the hardened pastes cured at 20 °C at early ages, which indicates that high temperature could improve the early hydration degrees of the hardened plain cement paste, the hardened composite binder containing copper slag and the hardened composite binder containing quartz powder. All binders have a relatively high hydration degree at 7 d. The non-evaporable water contents of the hardened plain cement paste and the hardened composite binder containing quartz powder increase very slowly, while the hardened composite binder containing copper slag has comparatively higher non-evaporable water content gain rates at late ages. These results indicate that although the hydration degree of cement is improved by high temperature at early ages, the hydration activity of cement cured at high temperature is

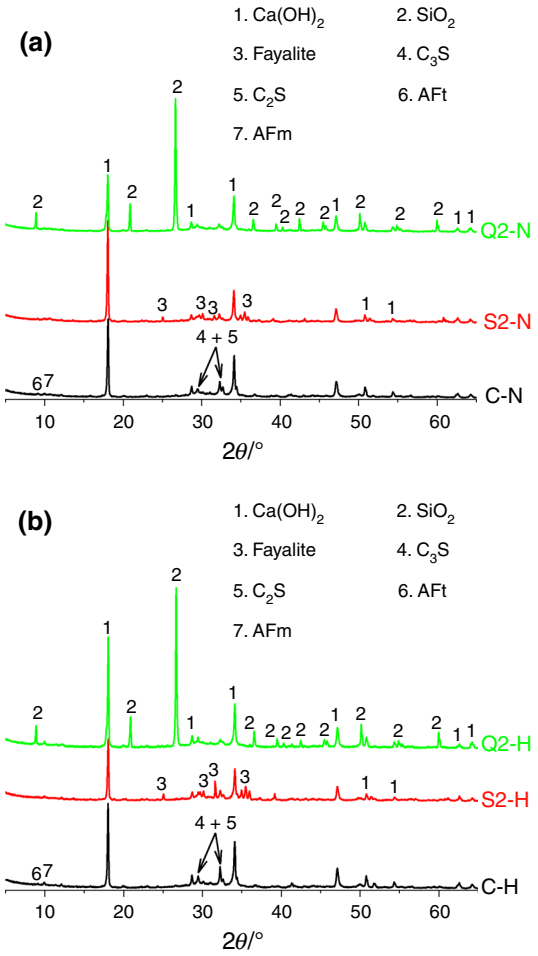

Fig. 9 XRD patterns of hardened pastes at 60 d. **a** standard curing; **b** high-temperature curing

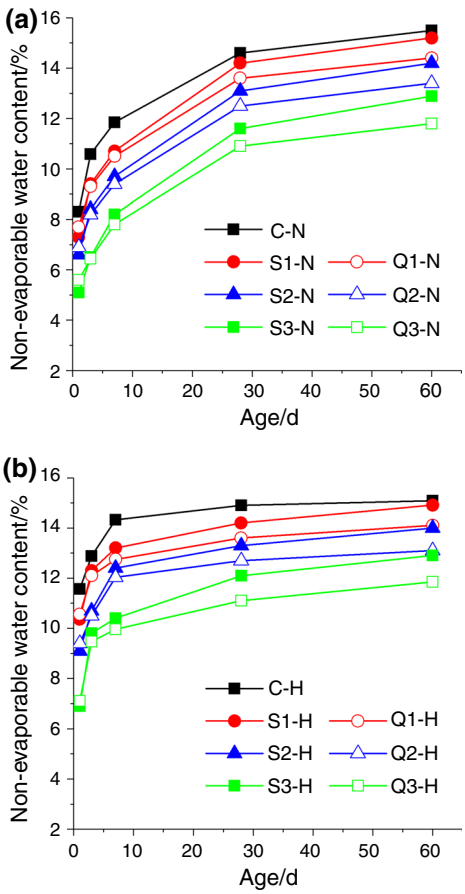

Fig. 10 **a** Non-evaporable water contents of hardened pastes under standard curing conditions. **b** Non-evaporable water contents of hardened pastes under high-temperature curing conditions

very low at late ages. However, the copper slag subjected to early high-temperature curing conditions has continuous hydration activity.

Compressive strength

Figure 11a shows the compressive strengths of mortars under standard curing conditions. The compressive strength gain rate of the mortar containing quartz powder is low, especially after 28 d. The compressive strength gain rate of the mortar containing copper slag is higher than that of the mortar containing quartz powder, and the compressive strength of the mortar containing copper slag is obviously higher than that of the mortar containing an equal mass quartz of powder at late ages. The quartz powder does not have hydration activity and acts as only filler in mortar. However, the copper slag, whose particle size distribution is similar to quartz powder, not only has a filling effect but also consumes $Ca(OH)_2$ and produces hydration products. In many studies, the compressive strength of concrete or mortar containing a pozzolanic material such as fly ash, silica fume or phosphorus slag is close to or even higher than that of plain cement or mortar without the pozzolanic material at late ages [9, 11, 43]. In this study, the compressive strength of the mortar containing copper slag is lower than that of plain cement mortar at 60 d, which also indicates that the pozzolanic activity of copper slag is relatively low.

Figure 11b shows the compressive strengths of mortars under high-temperature curing conditions. The early compressive strength of the mortar cured at 50 °C increases sharply compared with that of the mortar cured at 20 °C. The compressive strength of the mortar containing copper slag is obviously higher than that of the mortar containing quartz powder at early ages, which is different from the compressive strength results of mortars cured at 20 °C. This is because the hydration activity of copper slag is enhanced by high temperature. Furthermore, the compressive strength of the mortar containing copper slag is still obviously higher than that of the mortar containing quartz powder at 60 d.

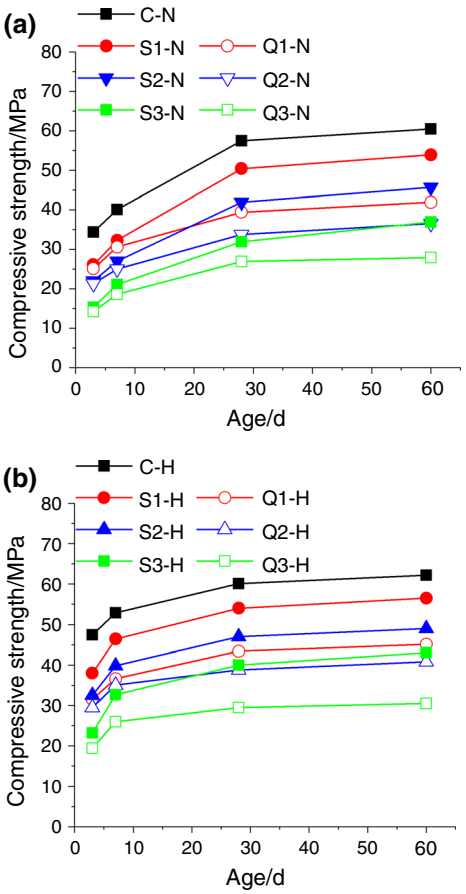

Fig. 11 **a** Compressive strengths of mortars under standard curing conditions. **b** Compressive strengths of mortars under high-temperature curing conditions

Conclusions

(1) Copper slag has a retarding effect on the hydration of cement, and this retarding effect becomes stronger with increasing copper slag content. Moreover, the retarding effect weakens at high temperatures.

(2) The addition of copper slag could reduce the hydration heat of the composite binder. Furthermore, the copper slag reacts partly and contributes to the hydration heat of the composite binder within 72 h at 20 °C and 50 °C.

(3) Copper slag has pozzolanic activity and consumes $Ca(OH)_2$ in hardened paste, although the pozzolanic activity of copper slag is low. The pozzolanic activity could be enhanced by high temperature. Moreover, the reaction of copper slag does not produce a new crystalline hydration product.

(4) The hardened composite binder containing copper slag has a higher non-evaporable water content gain rate than the hardened composite binder containing quartz powder at 20 °C and 50 °C. Additionally, the mortar containing copper slag has a higher compressive strength gain rate than the mortar containing quartz powder at 20 °C and 50 °C.

References

1. Han F, Wang Q, Liu M, Mei Y. Early hydration properties of composite binder containing limestone powder with different finenesses. J Therm Anal Calorim. 2016;123:1141–51.
2. Wang Q, Wang D, Zhuang S. The soundness of steel slag with different free CaO and MgO contents. Constr Build Mater. 2017;151:138–46.
3. Liu S, Kong Y, Wang L. A comparison of hydration properties of cement–low quality fly ash binder and cement–limestone powder binder. J Therm Anal Calorim. 2014;116:937–43.
4. Feng J, Liu S, Wang Z. Effects of ultrafine fly ash on the properties of high-strength concrete. J Therm Anal Calorim. 2015;121:1213–23.
5. Wang Q, Yang J, Chen H. Long-term properties of concrete containing limestone powder. Mater Struct. 2017;50:168.
6. Zhang T, Yu Q, Wei J, Li J. Investigation on mechanical properties, durability and micro-structural development of steel slag blended cements. J Therm Anal Calorim. 2012;110:633–9.
7. Zhang T, Yu Q, Wei J, et al. Study on optimization of hydration process of blended cement[J]. J Therm Anal Calorim. 2012;107:489–98.
8. Liu S, Li Q, Han W. Effect of various alkalis on hydration properties of alkali-activated slag cements. J Therm Anal Calorim. 2018;131:3093–104.
9. Hu J. Comparison between the effects of superfine steel slag and superfine phosphorus slag on the long-term performances and durability of concrete. J Therm Anal Calorim. 2017;128:1251–63.
10. Zhang T, Yu Q, Wei J, Zhang P, Chen P. Improvement of surface cementitious properties of coarse fly ash by dehydration and rehydration processes. J Therm Anal Calorim. 2012;109:265–71.
11. Wang Q, Wang D, Chen H. The role of fly ash microsphere in the microstructure and macroscopic properties of high-strength concrete. Cem Concr Compos. 2017;83:125–37.
12. Joshaghani A, Moeini MA, Balapour M, Moazenian A. Effects of supplementary cementitious materials on mechanical and durability properties of high-performance non-shrinking grout (HPNSG). J Sustain Cem-Based Mater. 2018;7:38–56.
13. Wang Q, Yan P, Mi G. Effect of blended steel slag-GBFS mineral admixture on hydration and strength of cement. Constr Build Mater. 2012;35:8–14.
14. Han F, Zhang Z, Liu J, Yan P. Effect of water-to-binder ratio on the hydration kinetics of composite binder containing slag or fly ash. J Therm Anal Calorim. 2017;128:855–65.
15. Han F, Zhang Z, Liu J, Yan P. Hydration kinetics of composite binder containing fly ash at different temperatures. J Therm Anal Calorim. 2016;124:1691–703.
16. Liu S, Xie G, Wang S. Effect of curing temperature on hydration properties of waste glass powder in cement-based materials. J Therm Anal Calorim. 2015;119:47–55.
17. Han F, Zhang Z. Hydration, mechanical properties and durability of high-strength concrete under different curing conditions. J Therm Anal Calorim. 2018;132:823–34.

18. Zhang Z, Wang Q, Chen H. Properties of high-volume limestone powder concrete under standard curing and steam-curing conditions. Powder Technol. 2016;301:16–25.
19. Gorai B, Jana RK. Characteristics and utilisation of copper slag-a review. Resour Conserv Recycl. 2003;39:299–313.
20. Geetha S, Madhavan S. High performance concrete with copper slag for marine environment. Mater Today: Proc. 2017;4:3525–33.
21. Sharma R, Khan RA. Influence of copper slag and metakaolin on the durability of self compacting concrete. J Clean Prod. 2017;171:1171–86.
22. Wu W, Zhang W, Ma G. Optimum content of copper slag as a fine aggregate in high strength concrete. Mater Design. 2010;31:2878–83.
23. Takebe H, Tomita S, Saitoh A, et al. Effect of crystallization on microstructure and elution properties in copper slag. J Sustain Metall. 2017;3:543–50.
24. Wang Z, Zhang T, Zhou L. Investigation on electromagnetic and microwave absorption properties of copper slag-filled cement mortar. Cem Concr Compos. 2016;74:174–81.
25. Chun T, Ning C, Long H, Li J, Yang J. Mineralogical characterization of copper slag from tongling nonferrous metals group China. JOM. 2016;68:2332–40.
26. Zuo Z, Yu Q, Wei M, Xie H, Duan W, Wang K, Qin Q. Thermogravimetric study of the reduction of copper slag by biomass. J Therm Anal Calorim. 2016;126:481–91.
27. Zuo Z, Yu Q, Xie H, Yang F, Qin Q. Thermodynamic analysis of reduction in copper slag by biomass molding compound based on phase equilibrium calculating model. J Therm Anal Calorim. 2018;132:1277–89.
28. Sarfo P, Das A, Wyss G, Young C. Recovery of metal values from copper slag and reuse of residual secondary slag. Waste Manage. 2017;70:272–81.
29. Raposeiras AC, Vargas-Cerón A, Movilla-Quesada D, Castro-Fresno D. Effect of copper slag addition on mechanical behavior of asphalt mixes containing reclaimed asphalt pavement. Constr Build Mater. 2016;119:268–76.
30. Behnood A, Gharehveran MM, Asl FG, Ameri M. Effects of copper slag and recycled concrete aggregate on the properties of CIR mixes with bitumen emulsion, rice husk ash, Portland cement and fly ash. Constr Build Mater. 2015;96:172–80.
31. Mavroulidou M. Mechanical properties and durability of concrete with water cooled copper slag aggregate. Waste Biomass Valor. 2017;8:1841–54.
32. Madheswaran CK, Ambily PS, Dattatreya JK, Rajamane NP. Studies on use of copper slag as replacement material for river sand in building constructions. J Inst Eng India Ser A. 2014;95:169–77.
33. Sharma R, Khan RA. Durability assessment of self compacting concrete incorporating copper slag as fine aggregates. Constr Build Mater. 2017;155:617–29.
34. Shi C, Meyer C, Behnood A. Utilization of copper slag in cement and concrete. Resour Conserv Recycl. 2008;52(10):1115–20.
35. Murari K, Siddique R, Jain KK. Use of waste copper slag, a sustainable material. J Mater Cycles Waste Manag. 2015;17:13–26.
36. Mag DA, Atc S, Andrade N. Blasted copper slag as fine aggregate in Portland cement concrete. J Environ Manag. 2017;196:607–13.
37. Najimi M, Sobhani J, Pourkhorshidi AR, DuEdwin RS, Gruyaert E, Belie ND. Influence of intensive vacuum mixing and heat treatment on compressive strength and microstructure of reactive powder concrete incorporating secondary copper slag as supplementary cementitious material. Constr Build Mater. 2017;155:400–12.
38. Mirhosseini SR, Fadaee M, Tabatabaei R, Fadaee MJ. Mechanical properties of concrete with Sarcheshmeh mineral complex copper slag as a part of cementitious materials. Constr Build Mater. 2017;134:44–9.
39. Najimi M, Sobhani J, Pourkhorshidi AR. Durability of copper slag contained concrete exposed to sulfate attack. Constr Build Mater. 2011;25:1895–905.
40. Moura WA, Gonçalves JP, Lima MBL. Copper slag waste as a supplementary cementing material to concrete. J Mater Sci. 2007;42:2226–30.
41. Chen Z, Yang EH. Early age hydration of blended cement with different size fractions of municipal solid waste incineration bottom ash. Constr Build Mater. 2017;156:880–90.
42. Weeks C, Hand RJ, Sharp JH. Retardation of cement hydration caused by heavy metals present in ISF slag used as aggregate. Cem Concr Res. 2008;30:970–8.
43. Zhang Z, Zhang B, Yan P. Comparative study of effect of raw and densified silica fume in the paste, mortar and concrete. Constr Build Mater. 2011;105:82–93.